Molecular Drivers of the Non-T Cell-Inflamed Tumor Microenvironment in Urothelial Bladder Cancer

Randy F. Sweis, M.D.[1], **Stefani Spranger, PhD.**[2], **Riyue Bao, PhD.**[3], **Gladell P. Paner, M.D.**[2], **Walter M. Stadler, M.D.**[1], **Gary Steinberg, M.D.**[4], and **Thomas F. Gajewski, M.D., PhD.**[1,2,*]

[1]Department of Medicine, Section of Hematology/Oncology, University of Chicago, Chicago, Illinois

[2]Department of Pathology, University of Chicago, Chicago, Illinois

[3]Center for Research Informatics, University of Chicago, Chicago, Illinois

[4]Department of Surgery, Section of Urology, University of Chicago, Chicago, Illinois

Abstract

Muscle-invasive urothelial bladder cancer is a common malignancy with poor outcomes for which immune checkpoint blockade is now showing promise. Despite clinical activity of PD-1/PD-L1-targeted therapy in this disease, most patients do not benefit and resistance mechanisms remain unknown. The non-T cell-inflamed tumor microenvironment correlates with poor prognosis and resistance to immunotherapies. In this report, we determined tumor-oncogenic pathways correlating with T cell exclusion. We first establish that T-cell-inflamed bladder tumors can be identified by immune gene expression profiling with concordance with CD8$^+$ T cell infiltration. Upregulation of genes encoding immune checkpoint proteins PD-L1, IDO, FOXP3, TIM3, and LAG3 was associated with T-cell-inflamed tumors, suggesting potential for sensitivity to checkpoint blockade. β-catenin, PPAR-γ, and FGFR3 pathways were activated in non-T cell-inflamed tumors. No difference was seen in overall somatic mutational density between groups. The three pathways identified represent targetable potential pathways of tumor-intrinsic immunotherapy resistance.

INTRODUCTION

Urothelial bladder cancer is the most common malignancy of the urinary system and estimated to cause 165,084 annual deaths worldwide (1). Despite chemotherapy, the outcomes for metastatic urothelial cancer remain poor with an overall 5-year survival rate of 15% (2). Given the need for novel approaches in this disease, the clinical exploration of immunotherapeutic checkpoint blockade is occurring rapidly (3-5). Inhibition of PD-1/PD-L1 interactions in bladder cancer has shown an objective response rate (ORR) of 52% in patients with tumor-infiltrating immune cells showing PD-L1 expression (6). Despite these

*Correspondence: University of Chicago Medicine, 5841 South Maryland Avenue, MC 2115, Chicago, IL 60637, Tel: +1-773-702-4601, Fax: +1-773-702-3163, tgajewsk@medicine.bsd.uchicago.edu.

promising data, the ORR rate in PD-L1-negative patients was just 11%. Thus, the majority of urothelial cancer patients do not benefit from immune checkpoint blockade and mechanisms of resistance remain incompletely understood.

The presence of an existing antitumor T cell response in all cancers is important for the activity of immunotherapies, including checkpoint blockade (7,8). Tumors with a T-cell-inflamed microenvironment are characterized by infiltration of CD8^{+} T cells, chemokines, and an interferon signature, which are associated with improved survival and response to immunotherapies (9-12). In urothelial bladder cancer, increased T cell infiltration has been correlated with longer patient survival (13). Efforts have now been focused on understanding mechanisms driving T cell exclusion. Recently, β-catenin activation has been identified in melanoma as the first tumor oncogenic pathway leading to a non-T cell-inflamed phenotype (14). Stabilization of β-catenin leads to ATF3-dependent transcriptional repression of CCL4, which ablates recruitment of Batf3-lineage dendritic cells into the tumor microenvironment. This, in turn, leads to failed T cell priming, defective T cell recruitment, and loss of therapeutic response to anti-PD-L1 and anti-CTLA-4 therapies in a murine model. In other cancer types, it is not yet known whether the same or additional tumor-intrinsic signaling pathways affect the development of a T-cell-inflamed phenotype. We therefore pursued the identification of pathways and mutations associated with non-T cell-inflamed urothelial bladder tumors to discover new candidate therapeutic targets for improving immunotherapy efficacy.

MATERIALS AND METHODS

Identification of T-cell-inflamed and non-T cell-inflamed subtypes in TCGA

The Cancer Genome Atlas (TCGA) Bladder Urothelial Carcinoma (BLCA) RNA-seq gene expression data were downloaded from Broad Genome Data Analysis Center (http://gdac.broadinstitute.org, release date 07/15/2014) as previously described (14). The upper quartile-normalized and log_2-transformed RNA-seq by expectation maximization (RSEM) values for 267 samples were summarized at gene level (15). Genes expressed in <80% of the samples were filtered. Exome somatic mutation data were downloaded from TCGA portal (11/16/2014) for 238 tumor-normal-sample pairs with variants from "BI Automated Mutation Calling".

Unsupervised hierarchical clustering using R function hclust v3.1.0 with K equal to 10 was conducted on 16,197 genes. A 725 gene cluster contained 12 from our previously described T cell signature (CD8A, CCL2, CCL3, CCL4, CXCL9, CXCL10, ICOS, GZMK, HLA-DMA, HLA-DMB, HLADOA, HLA-DOB). Consensus clustering of the primary tumor samples was performed using BioConductor package ConsensusClusterPlus v1.18.0 (16) based on expression of the 725 genes, with 2,000 re-sampling cycles, using hierarchical clustering and Euclidean distance. Three distinct tumor subtypes were identified, with low, moderate, and high expression level of the T cell genes (Fig. 1A). PCA mapping showed separation of subtypes.

Characterization of activated pathways and differentially mutated genes

Genes differentially expressed between tumor groups were detected from the global set of 16,197 genes by using ANOVA and filtered by false discovery rate (FDR) q-value < 0.01 and fold change 2.0 (or −2.0). Canonical pathways significantly enriched in the genes of interest were identified by Ingenuity Pathways Analysis (Ingenuity Systems; http://www.ingenuity.com) based on experimental evidence from the Ingenuity Knowledge Base (3/23/2014). A total of 78,762 somatic variants were converted to VCF format and annotated with exonic function, population frequency, dbSNP, COSMIC database, and deleterious function prediction. Synonymous variants, those with no annotation available, and those with a population frequency >1% were filtered. The resulting 55,996 variants were kept for further analysis. The variants were then summarized at gene- and patient- level for comparison of mutation profiles between groups. SNVs located in selected genes were analyzed using the SIFT prediction algorithm (http://sift.jcvi.org/) (17).

Immunohistochemistry

The immunohistology staining on human bladder tumors was performed by the Human Tissue Resource Center (HTRC) at the University of Chicago using tissue from cystectomy specimens from muscle-invasive bladder cancer, corresponding to specimens previously submitted for inclusion in TCGA. Staining was performed using a CD8-specific monoclonal antibody (CD8 clone C8/144B, NeoMarkers) and a β-catenin monoclonal antibody (clone CAT-5H1, Life Technologies) in combination with a secondary goat anti-mouse immunoglobulin G (IgG) conjugated to an alkaline phosphatase (Biocare Medical). Slides were scanned using a CRi Panoramic Scan Whole Slide Scanner and viewed with Pannoramic Viewer 1.15.4 (3DHISTECH). CD8$^+$ cells from three 0.1 mm^2 fields were counted manually and averaged. Tumors were considered positive for intratumoral T cells if >1 CD8$^+$ cell was present. For β-catenin, tumors with any nuclear staining were considered positive. A urologic pathologist (G.P.) scored samples for intensity and distribution in a blinded fashion.

RESULTS

Classifying subtypes of urothelial bladder cancer by immune gene profiling

We first aimed to determine whether T-cell-inflamed and non-T cell-inflamed bladder tumors could be identified using immune gene expression profiling. Genes from a previously derived T-cell signature were used to classify 267 samples of urothelial bladder cancer analyzed from The Cancer Genome Atlas (TCGA) (7,10). First, unsupervised hierarchical clustering was conducted on 16,197 genes. A cluster of 725 genes contained 12 genes from the T-cell signature was used to perform consensus clustering of tumor samples, which identified groups with high, intermediate, and low expression of the immune genes (Fig. 1A). Those groups were compared to identify pathways linked with the non-T cell-inflamed tumor microenvironment. The non-T cell-inflamed group was comprised of 88 samples (33%), whereas the T-cell-inflamed group represented 95 samples (36%). The remainder of samples showed intermediate expression of the T-cell signature genes. Thus, like metastatic melanoma, bladder cancers could be segregated based on the degree of expression of genes indicative of a T-cell-inflamed tumor microenvironment (14).

T-cell-inflamed cancers overexpressed inhibitory molecules and were infiltrated by T cells

In order to validate the correlation between the T-cell-inflamed tumor microenvironment gene signature and actual presence of intratumoral T cells, a subset of 19 TCGA samples derived from our institution was analyzed by immunohistochemistry (IHC) for CD8. We found that 37% of samples showed a notable absence of intratumoral CD8^{+} T cells, whereas 63% showed significant CD8^{+} T-cell infiltration (Fig. 1B). T-cell infiltrated tumors contained a median of 14 CD8^{+} T cells per high power field (range 2-47). Comparison between IHC and gene expression profiling revealed that the presence of intratumoral CD8^{+} T cells was strongly associated with the T-cell-inflamed gene expression signature ($P = 0.01$, Fig. 1C).

In other cancers, expression of immune inhibitory molecules has been linked with a T-cell-inflamed phenotype (9). Therefore, we evaluated the expression of inhibitory molecules in bladder cancers and examined for correlation with the T cell signature. Expression of PD-L1 mRNA positively correlated with that of CD8A ($P < 0.0001$, Fig. 2A), and the T-cell-inflamed tumors had higher expression of both genes as compared to the non-T cell-inflamed tumors. A similar positive correlation was observed with other immune-inhibitory markers IDO, FOXP3, TIM3, and LAG3 (Fig. 2B). As in melanoma, T-cell-inflamed bladder cancers are characterized by the highest expression of genes that reflect negative feedback pathways that limit ongoing T cell activation.

Non-T cell-inflamed tumors have activated β-catenin and PPAR-γ

Identification of molecular pathways active in tumor cells that might mediate T-cell exclusion from the tumor microenvironment has become a high priority as we move towards developing new therapeutic interventions to expand the fraction of patients responding to immunotherapies. Based on the recent characterization of the Wnt/β-catenin pathway in melanoma as being causal for preventing T-cell activation and trafficking into the tumor microenvironment (14), we pursued a similar analysis in bladder cancer. To identify pathways linked to the non-T cell-inflamed phenotype, we compared gene expression patterns between T-cell-inflamed and non-T cell-inflamed bladder cancers. We found 3,112 genes differentially expressed between the two groups ($Q < 0.01$, Supplementary Table S1), with 730 being preferentially expressed in the non-T cell-inflamed tumors. We focused on the latter set of genes and evaluated for pathway enrichment using Ingenuity Pathways Analysis. The top activated upstream regulators identified were β-catenin and PPAR-γ (both $P = 0.003$). Thirty genes related to β-catenin signaling and 22 genes related to PPARG-γ were overexpressed in the non-T cell-inflamed tumors (Fig. 3A-B).

We further explored the two pathways by evaluating gene expression of PPARG and of WNT7B, the primary ligand associated with β-catenin signaling in melanoma (14). Both genes showed an inverse correlation with expression of CD8A ($P < 0.0001$), further suggesting a link between activation of those pathways and the absence of intratumoral T cells. To confirm this pattern at the protein level, we used immunohistochemistry to examine expression of stabilized β-catenin versus extent of CD8^{+} T cell infiltration. Indeed, an inverse relationship was observed between nuclear staining of β-catenin and the presence of

intratumoral CD8$^+$ T cells (P = 0.036, Fig. 3C-D). Nuclear staining was only found in samples without intratumoral CD8$^+$ T cells, although only accounted for 43% of the non-T cell-inflamed tumors. These results are consistent with what was observed in melanoma, in which 48% of the non-T cell-inflamed tumors showed β-catenin pathway activation (14).

To assess a potential underlying mechanism of T-cell exclusion in this tumor type, we evaluated expression of the chemokine CCL4 and the transcription factor BATF3, which are associated with recruitment of the critical population of dendritic cells necessary for T-cell activation in the melanoma context (14). CD8 transcripts were correlated with CCL4 and BATF3 expression within the tumor microenvironment (Supplementary Fig. S1A). We confirmed the expected inverse correlation with WNT7B expression, but also found that PPARG showed the same relative expression pattern (Supplementary Fig. S1B). Thus, the recruitment of BATF3-lineage dendritic cells necessary for cross presentation of tumor antigens might also be negatively influenced by PPARG. Lastly, of the 29 β-catenin target genes overexpressed in our dataset, only IHH and GATA2 overlapped with the 22 target genes of PPARG. Despite this lack of overlap, target gene expression for both pathways was strongly correlated (P < 0.0001), indicating a potential synergistic mechanism of immune exclusion.

Mutated FGFR3 and coactivators of PPAR-γ in non-T cell-inflamed cancers

We next interrogated somatic mutations between T-cell-inflamed and non-T cell-inflamed subtypes to identify mutations in pathways that might be exclusive to the non-T cell-inflamed subset. Analysis of exome sequencing data revealed no difference in the overall number of nonsynonymous mutations per patient for each group (P = 0.80). Thus, a lower mutational density alone could not explain the absence of T cells in a major subset of tumors. We therefore reviewed differential mutations at the individual gene level. We found 891 genes mutated in two or more samples exclusive to non-inflamed tumors (Supplementary Table S2). FGFR3 was the most common mutation exclusive to non-inflamed tumors (P < 0.0001). Fourteen separate FGFR3 mutations were detected in 11 of the non-T cell-inflamed samples, with no mutations detected in the T-cell-inflamed samples. Nine unique mutations were identified (Table 1) and two were recurrent (G370C in 3 samples and Y373C in 4 samples). The two most common FGFR3 mutations, Y373C and G370C, have been reported previously in bladder cancer and lead to activation of the receptor through increased ligand-independent dimerization and phosphorylation (18). Additionally, recurrent in-frame activating FGFR3-TACC3 fusions were found exclusively in non-T cell-inflamed tumors (3 samples). We also analyzed FGFR3 gene expression and found an inverse correlation with expression of CD8A (P < 0.0001). Non-T cell-inflamed tumors showed higher expression of FGFR3 as compared to the T-cell-inflamed tumors.

Finally, we also discovered that PPARGC1A and PPARGC1B were exclusively mutated in non-T cell-inflamed tumors. Both are coactivators of PPAR-γ, which was one of the top activated regulators in our gene expression pathway analysis. PPARGC1A mutations included A728D, C726Y, K663*, R657Q, R485W, and R408T. PPARGC1B mutations included P607L, V703I, E787K, and S994L. These mutations were evaluated by a prediction algorithm, Sorting Tolerant From Intolerant (SIFT), and seventy-percent were predicted to

affect protein function (17). Together, these data identify the β-catenin pathway, the PPAR-γ pathway, and active FGFR3 as three potential cancer-intrinsic pathways that could contribute to T cell exclusion in bladder cancer.

DISCUSSION

Using our immune gene signature, we found that urothelial bladder cancer segregated into T-cell-inflamed and non-T cell-inflamed subtypes, and the latter phenotype correlates with an absence of CD8^{+} T cells by IHC. Unsupervised clustering analyses of muscle invasive bladder cancer based on global gene expression segregates tumors into two to four intrinsic subtypes (19-21), but previous studies did not evaluate segregation based on T-cell infiltration in bladder cancer, as we have done. Our strategy was based on the presence of immune cells in the tumor microenvironment, rather than clustering by tumor-derived genomic pathways. Although the latter approach might better identify chemotherapeutic resistance pathways, the former is more likely to yield insight into immunotherapy resistance. PPAR-γ pathway activation and FGFR3 mutations are associated with the "luminal" intrinsic bladder subtype, and we found both were also linked with the non-T cell-inflamed phenotype. Further bioinformatic and experimental analyses is needed to determine the relationship of the non-T cell-inflamed subtype and previously described bladder cancer intrinsic subtypes.

Our use of immune gene expression profiling identified three molecular pathways linked with the non-T cell-inflamed subtype. Our methodology selected for genes overexpressed in tumors with an absence of immune infiltrating cells, which by inference were highly likely to arise from tumor-intrinsic activated molecular pathways. Modulation of these targets could prove useful to overcome primary resistance to immune checkpoint blockade such as PD-1/PD-L1-targeted therapies. One limitation to this analysis is its correlative nature. However, similar methodology has resulted in the discovery a causal link between activated β-catenin and intratumoral T-cell restriction via ATF3-mediated CCL4 repression in melanoma, which was, indeed, confirmed through careful experimental studies in genetically engineered mouse models (14). Our study independently validated this pathway as active in non-T cell-inflamed bladder cancers. We also identified two other molecular pathways not previously found in melanoma. The effect of modulation of these pathways on the induction of a T-cell-inflamed phenotype will be attractive to pursue in future studies. The availability of FGFR3 inhibitors for clinical testing provides a rationale and feasibility for combination with monoclonal antibodies to PD-1 or PD-L1.

Understanding the non-T cell-inflamed phenotype in urothelial bladder, as well as other cancers, is critical to improving response rates for future immunotherapeutic development (22,23). Three immune checkpoint inhibitors have been approved by the FDA since 2011 for melanoma, renal, and non-small cell lung cancers (23-25). It is critical to continue advancing our biologic understanding of tumors with primary resistance to expand the proportion of patients responding to these immunotherapies. A better understanding of resistance will catalyze the development of new clinical trial strategies s with combination therapies that overcome resistance in urothelial bladder cancer and, ultimately, other tumor types.

Supplementary Material

Refer to Web version on PubMed Central for supplementary material.

REFERENCES

1. Ferlay J, Soerjomataram II, Dikshit R, Eser S, Mathers C, Rebelo M, et al. Cancer incidence and mortality worldwide: sources, methods and major patterns in GLOBOCAN 2012. International Journal Of Cancer Journal International Du Cancer. 2014

2. von der Maase H, Sengelov L, Roberts JT, Ricci S, Dogliotti L, Oliver T, et al. Long-term survival results of a randomized trial comparing gemcitabine plus cisplatin, with methotrexate, vinblastine, doxorubicin, plus cisplatin in patients with bladder cancer. J Clin Oncol. 2005; 23(21):4602–8. [PubMed: 16034041]

3. Bracarda S, Altavilla A, Hamzaj A, Sisani M, Marrocolo F, Del Buono S, et al. Immunologic checkpoints blockade in renal cell, prostate, and urothelial malignancies. Semin Oncol. 2015; 42(3): 495–505. [PubMed: 25965369]

4. Carosella ED, Ploussard G, LeMaoult J, Desgrandchamps F. A Systematic Review of Immunotherapy in Urologic Cancer: Evolving Roles for Targeting of CTLA-4, PD-1/PD-L1, and HLA-G. Eur Urol. 2015; 68(2):267–79. [PubMed: 25824720]

5. Kim JW, Tomita Y, Trepel J, Apolo AB. Emerging immunotherapies for bladder cancer. Curr Opin Oncol. 2015; 27(3):191–200. [PubMed: 25811346]

6. Powles T, Eder JP, Fine GD, Braiteh FS, Loriot Y, Cruz C, et al. MPDL3280A (anti-PD-L1) treatment leads to clinical activity in metastatic bladder cancer. Nature. 2014; 515(7528):558–62. [PubMed: 25428503]

7. Harlin H, Meng Y, Peterson AC, Zha Y, Tretiakova M, Slingluff C, et al. Chemokine expression in melanoma metastases associated with CD8+ T-cell recruitment. Cancer Res. 2009; 69(7):3077–85. [PubMed: 19293190]

8. Ji RR, Chasalow SD, Wang L, Hamid O, Schmidt H, Cogswell J, et al. An immune-active tumor microenvironment favors clinical response to ipilimumab. Cancer Immunol Immunother. 2012; 61(7):1019–31. [PubMed: 22146893]

9. Spranger S, Spaapen RM, Zha Y, Williams J, Meng Y, Ha TT, et al. Up- regulation of PD-L1, IDO, and T(regs) in the melanoma tumor microenvironment is driven by CD8(+) T cells. Sci Transl Med. 2013; 5(200):200ra116.

10. Gajewski TF, Louahed J, Brichard VG. Gene signature in melanoma associated with clinical activity: a potential clue to unlock cancer immunotherapy. Cancer J. 2010; 16(4):399–403. [PubMed: 20693853]

11. Gajewski TF, Schreiber H, Fu YX. Innate and adaptive immune cells in the tumor microenvironment. Nat Immunol. 2013; 14(10):1014–22. [PubMed: 24048123]

12. Gajewski TF, Woo SR, Zha Y, Spaapen R, Zheng Y, Corrales L, et al. Cancer immunotherapy strategies based on overcoming barriers within the tumor microenvironment. Curr Opin Immunol. 2013; 25(2):268–76. [PubMed: 23579075]

13. Sharma P, Shen Y, Wen S, Yamada S, Jungbluth AA, Gnjatic S, et al. CD8 tumor-infiltrating lymphocytes are predictive of survival in muscle-invasive urothelial carcinoma. Proc Natl Acad Sci U S A. 2007; 104(10):3967–72. [PubMed: 17360461]

14. Spranger S, Bao R, Gajewski TF. Melanoma-intrinsic β-catenin signalling prevents anti-tumour immunity. Nature. 2015; 523(7559):231–5. [PubMed: 25970248]

15. Li B, Dewey CN. RSEM: accurate transcript quantification from RNA-Seq data with or without a reference genome. BMC Bioinformatics. 2011; 12:323. [PubMed: 21816040]

16. Wilkerson MD, Hayes DN. ConsensusClusterPlus: a class discovery tool with confidence assessments and item tracking. Bioinformatics. 2010; 26(12):1572–3. [PubMed: 20427518]

17. Kumar P, Henikoff S, Ng PC. Predicting the effects of coding non-synonymous variants on protein function using the SIFT algorithm. Nat Protoc. 2009; 4(7):1073–81. [PubMed: 19561590]

18. Iyer G, Milowsky MI. Fibroblast growth factor receptor-3 in urothelial tumorigenesis. Urol Oncol. 2013; 31(3):303–11. [PubMed: 22285006]

19. Choi W, Porten S, Kim S, Willis D, Plimack ER, Hoffman-Censits J, et al. Identification of distinct basal and luminal subtypes of muscle-invasive bladder cancer with different sensitivities to frontline chemotherapy. Cancer Cell. 2014; 25(2):152–65. [PubMed: 24525232]

20. Network CGAR. Comprehensive molecular characterization of urothelial bladder carcinoma. Nature. 2014; 507(7492):315–22. [PubMed: 24476821]

21. Damrauer JS, Hoadley KA, Chism DD, Fan C, Tiganelli CJ, Wobker SE, et al. Intrinsic subtypes of high-grade bladder cancer reflect the hallmarks of breast cancer biology. Proc Natl Acad Sci U S A. 2014; 111(8):3110–5. [PubMed: 24520177]

22. Gajewski TF. The Next Hurdle in Cancer Immunotherapy: Overcoming the Non- T Cell-inflamed Tumor Microenvironment. Seminars in Oncology.

23. Hamid O, Robert C, Daud A, Hodi FS, Hwu WJ, Kefford R, et al. Safety and tumor responses with lambrolizumab (anti-PD-1) in melanoma. N Engl J Med. 2013; 369(2):134–44. [PubMed: 23724846]

24. Hodi FS, O'Day SJ, McDermott DF, Weber RW, Sosman JA, Haanen JB, et al. Improved survival with ipilimumab in patients with metastatic melanoma. N Engl J Med. 2010; 363(8):711–23. [PubMed: 20525992]

25. Brahmer J, Reckamp KL, Baas P, Crinò L, Eberhardt WE, Poddubskaya E, et al. Nivolumab versus Docetaxel in Advanced Squamous-Cell Non-Small-Cell Lung Cancer. N Engl J Med. 2015; 373(2):123–35. [PubMed: 26028407]
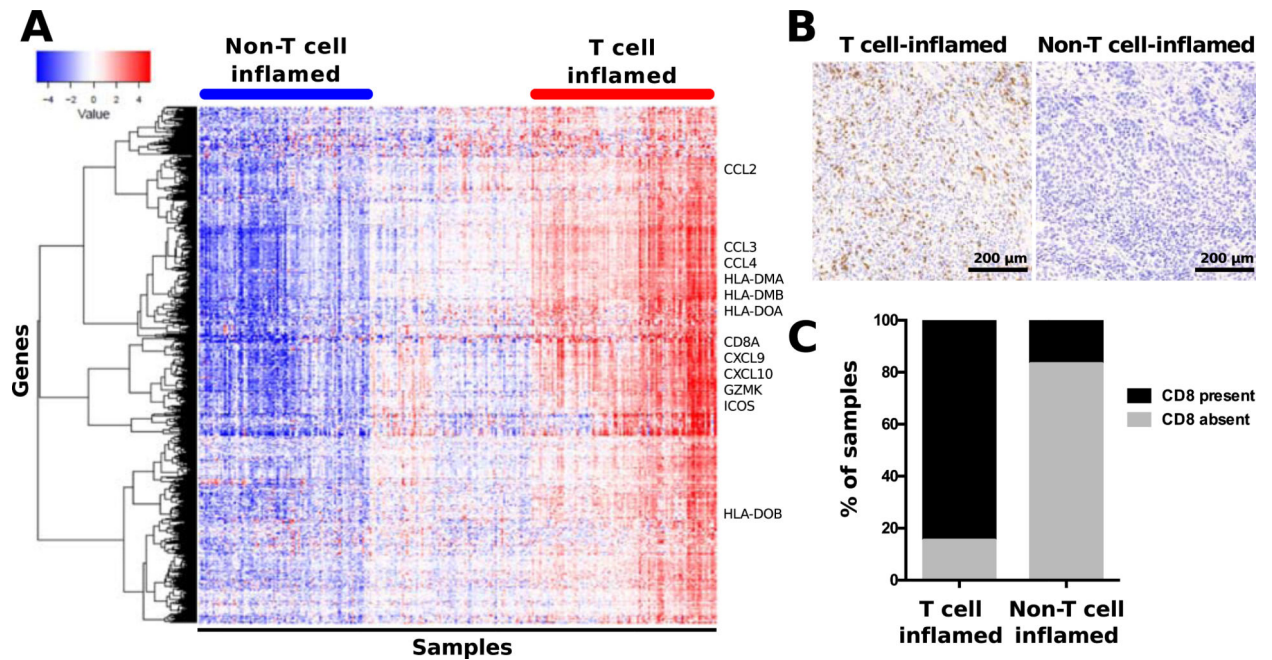
Figure 1.
(A) T cell-inflamed and non-T cell-inflamed bladder tumors can be distinguished by immune gene expression profiling. Eighty-eight (33%) of tumors show minimal expression of T cell related immune genes (non-T cell-inflamed) while 95 (36%) show overexpression (T cell-inflamed). The remainders show a mixed expression pattern of T cell related genes. (B) Representative examples of CD8 immunohistochemical staining showing an absence of intratumoral T cells in a non-T cell-inflamed tumor (left) and marked T cell infiltration in a T-cell-inflamed tumor (right). (C) Immune subtypes identified by immune gene expression profiling show significant association with the presence of T cells by immunohistochemistry, defined as having >1 CD8+ T cell per 0.1 mm^2 field ($P = 0.01$, Fisher's exact test, $n = 19$).
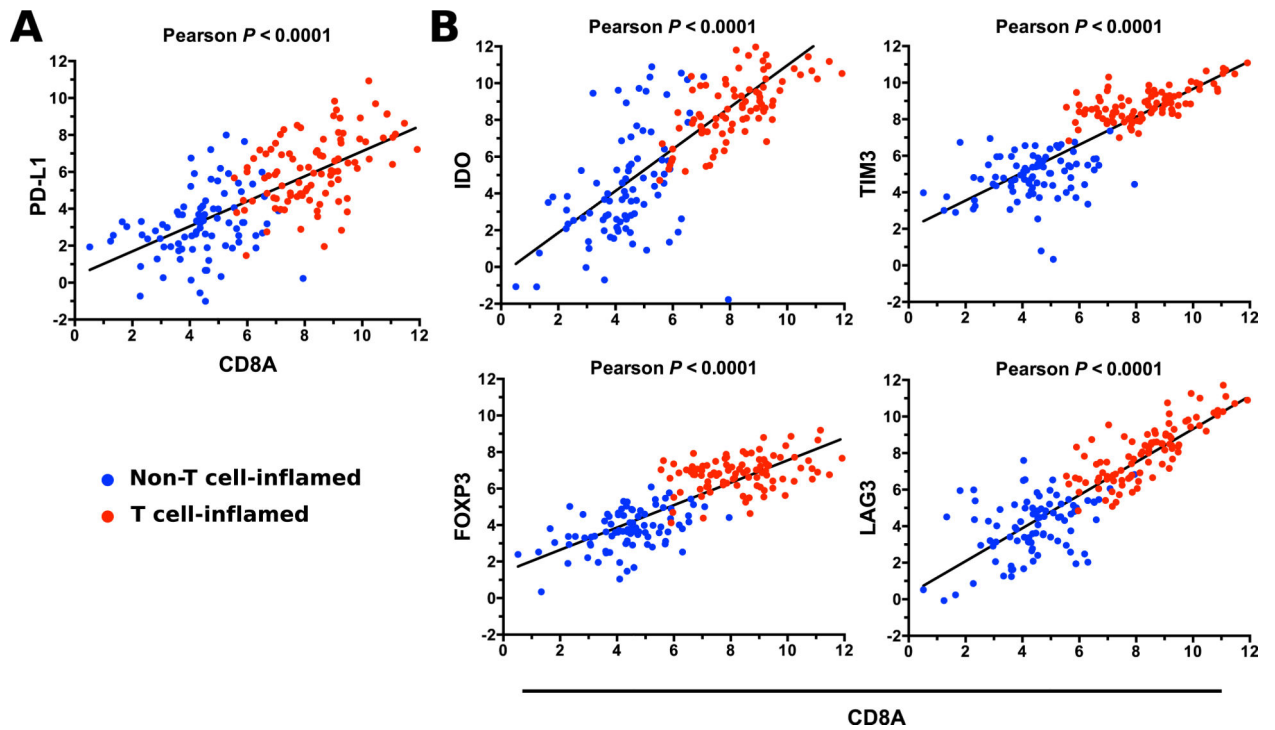
Figure 2.
(A) Expression of PD-L1 is positively correlated with expression of CD8A (*P* < 0.0001, Pearson correlation). T cell-inflamed tumors (red) show higher expression of both genes compared with non-T cell-inflamed tumors (blue). (B) Additional immune inhibitory molecules, IDO1, FOXP3, TIM3, and LAG3 show a similar significant correlation (all *P* < 0.0001, Pearson correlation).
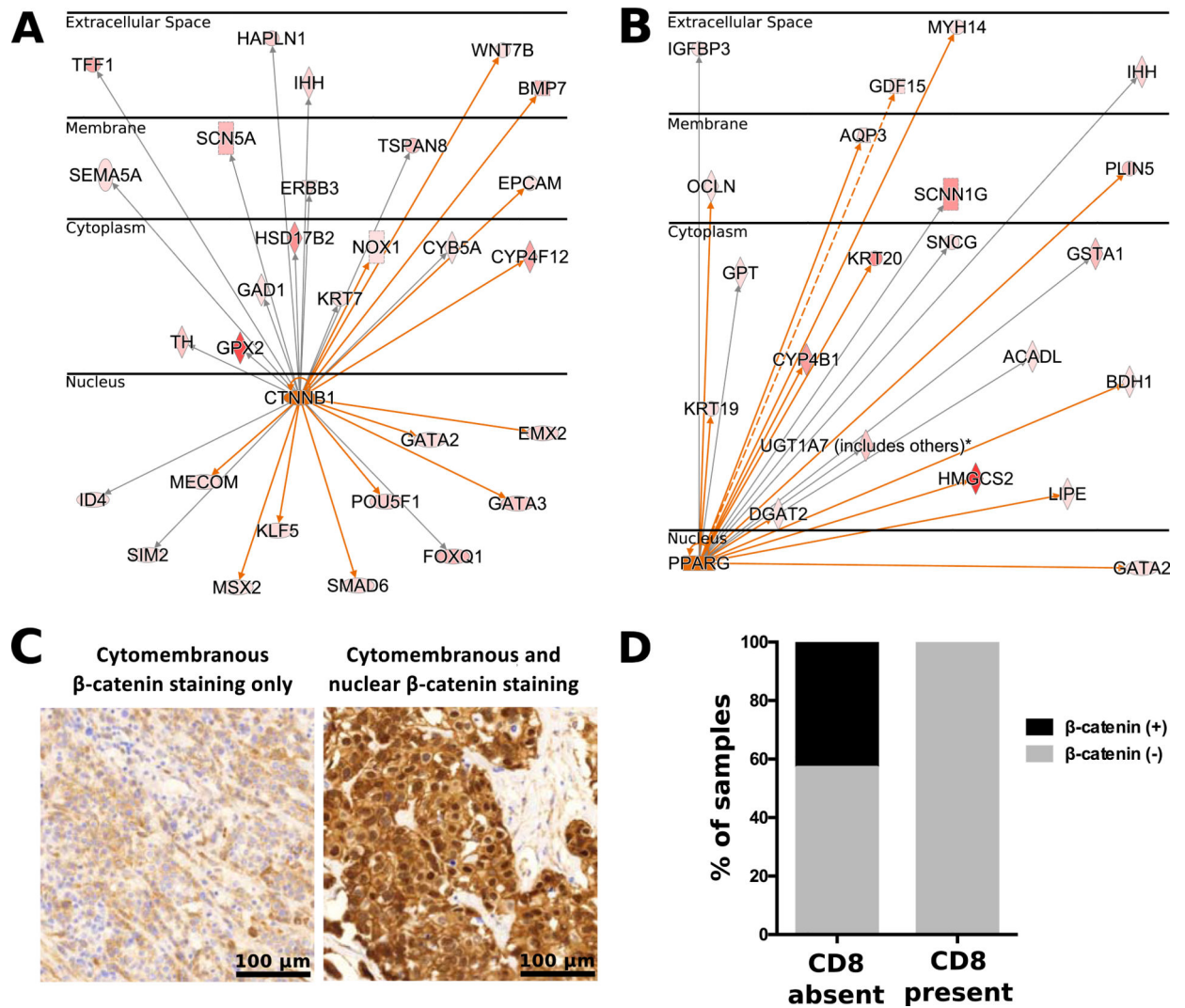
Figure 3.
Cellular localization of molecules upregulated in the non-T cell-inflamed group and their relationship with (A) β-catenin and (B) PPARG. Arrows point from the regulator towards a molecule being regulated. Intensity of red color is proportional to level of upregulation. Dotted lines indicate indirect relationships. Lines highlighted in orange show predicted activation. (C) All bladder tumors showed cytomembranous staining for β-catenin (left), however a fraction of non-T cell-inflamed tumors showed nuclear staining for β-catenin (right). (D) Nuclear β-catenin staining was only found in tumors with an absence of CD8+ T cells ($P = 0.036$, Fischer's exact test, $n = 19$).

Table 1

FGFR3 mutations found in non-T cell-inflamed bladder cancers.

TCGA Sample ID	Mutation	Amino Acid Substitution
TCGA-DK-A3IS-01	chr4:1803377:G:A	E216K
TCGA-DK-A3IS-01	chr4:1803395:G:A	D222N
TCGA-DK-A3IS-01	chr4:1803435:G:A	G235D
TCGA-FJ-A3ZF-01	chr4:1803738:G:A	V306I
TCGA-GU-A42R-01	chr4:1805533:C:T	H349Y
TCGA-UY-A78N-01	chr4:1805561:C:T	P358L
TCGA-CF-A5U8-01		
TCGA-E7-A3Y1-01	chr4:1806089:G:T	G370C
TCGA-E7-A7DU-01		
TCGA-BT-A42C-01		
TCGA-CF-A47W-01	chr4:1806099:A:G	Y373C
TCGA-DK-A6B0-01		
TCGA-E7-A5KF-01		
TCGA-DK-A3IS-01	chr4:1808937:C:-:	A790fs
	Fusions	
TCGA-CF-A3MF-01		
TCGA-CF-A3MG-01	FGFR3-TACC3	
TCGA-CF-A3MH-01		